

# X-ray photoelectron spectroscopy and Auger electron spectroscopy analyses of the initial growth mechanism of CdTe layers on (100) GaAs by metalorganic vapor phase epitaxy

Mitsuru Ekawa, Kazuhito Yasuda, Syuji Sone, Yoshiyuki Sugiura, and Manabu Saji  
*Department of Electrical and Computer Engineering, Nagoya Institute of Technology, Gokiso-cho, Showa-ku, Nagoya 466, Japan*

Akikazu Tanaka

*Electronics Materials Laboratory, Sumitomo Metal Mining Co., Ltd., Suehiro-cho, Ohme-shi, Tokyo 198, Japan*

(Received 2 January 1990; accepted for publication 30 January 1990)

X-ray photoelectron spectroscopy and Auger electron spectroscopy measurements were performed to investigate the initial growth mechanism and the selection of growth orientations of CdTe layers grown on (100) GaAs by metalorganic vapor phase epitaxy (MOVPE). The surface stoichiometry of the GaAs substrate was found to recover when annealed in a H<sub>2</sub> flow atmosphere (500 °C, 5 min), although the surface was initially in an As-rich condition after chemical etching by H<sub>2</sub>SO<sub>4</sub>:H<sub>2</sub>O<sub>2</sub>:H<sub>2</sub>O = 5:1:1. No oxide was observed at both the etched and H<sub>2</sub> annealed GaAs surfaces. Preferential adsorption of Te occurred on the GaAs surface when H<sub>2</sub> annealing was carried out in the growth reactor in the presence of residual CdTe deposits. One monolayer of Te with a thickness of about 1.8 Å was adsorbed on the GaAs surface when the H<sub>2</sub> annealed GaAs was exposed to diethyltelluride during the cooling period from the annealing temperature to the growth temperature (420 °C). On the other hand, minimal adsorption of Cd occurred when the H<sub>2</sub> annealed GaAs was exposed to dimethylcadmium during the above period. (100) CdTe growth was reproducibly achieved when the GaAs surface was completely covered by one monolayer of Te before growth, otherwise (111) growth occurred. Differences in the initial growth mechanism between MOVPE and molecular-beam epitaxy are also discussed.

## I. INTRODUCTION

The epitaxial growth of CdTe and HgCdTe on (100) GaAs substrates is now of great interest since this system is promising for the large-scale integrated infrared detectors.<sup>1-4</sup> Metalorganic vapor phase epitaxy (MOVPE) and molecular-beam epitaxy (MBE) have been the major growth techniques to fabricate such systems. However, it has been known that growth can proceed in two different growth orientations of (100) and (111) due to a large lattice mismatch (~15%) between the GaAs substrate and the grown layer.<sup>5-10</sup> The selection of growth orientations has been extensively studied in MBE, and several mechanisms have been proposed. For instance, it has been suggested that (100) growth occurs when an oxide remains on the GaAs surface.<sup>11-13</sup> The adsorption of Te on the GaAs surface has also been considered to be a factor influencing the CdTe orientation.<sup>14-16</sup> In MOVPE, on the other hand, similar orientation characteristics have been observed,<sup>17</sup> however, little effort has been devoted to clarify the initial growth mechanism.

There are considerable differences in the preparation procedures of GaAs substrates before growth between MBE and MOVPE. In MBE, substrate soldering on the sample holder with indium is commonly performed to achieve the thermal contact,<sup>18</sup> and this procedure is known to produce an oxide layer on the substrate.<sup>19</sup> In order to remove the surface oxide, preheating of the GaAs substrates is usually carried out around 580 °C under high vacuum, however, this process results in a deviation of surface stoichiometry of the

substrates, due to the evaporation of As. In MOVPE, on the other hand, such an oxidation process can be avoided and growth proceeds in a deoxidizing H<sub>2</sub> atmosphere. Thus, the initial growth mechanism may differ between MOVPE and MBE.

Previously, we performed XPS analysis of GaAs surface structures to clarify the initial growth mechanism of CdTe layers on GaAs in MOVPE.<sup>20,21</sup> In this paper, we report the results obtained in systematic XPS and AES analyses which were carried out on (100) GaAs at each stage of the pretreatment procedures in CdTe growth by MOVPE. Additional AES measurements have revealed the details of the GaAs surface structures before growth, and the adsorption characteristics of the precursors. The variations of GaAs surface structures in the MOVPE process are definitively discussed in contrast to the MBE process. The key to controlling the orientations of CdTe layers is also clarified.

## II. EXPERIMENTAL PROCEDURES

CdTe growth was carried out in a low-pressure MOVPE system operating at 60 Torr. The metalorganic sources used were dimethylcadmium (DMCd) and diethyltelluride (DETe), which were delivered to the growth reactor using palladium-diffused H<sub>2</sub> as a carrier gas. The flow rates of DMCd and DETe were  $2 \times 10^{-5}$  and  $8 \times 10^{-5}$  mol/min, respectively. The total flow rate of H<sub>2</sub> was 1 SLM. The growth temperature was 420 °C which is compatible with the subsequent growth of HgCdTe for the use of DETe.

In this study, both semi-insulating and  $n^+$  GaAs were

used as the substrates, and these were exactly (100) oriented. After degreasing, the substrates were etched in a solution of  $\text{H}_2\text{SO}_4:\text{H}_2\text{O}_2:\text{H}_2\text{O} = 5:1:1$  for 5 min, rinsed with deionized water and then rinsed with methanol and isopropyl alcohol. After the last rinse, the substrates were immediately loaded into the growth reactor. Prior to growth, these substrates were annealed at  $500^\circ\text{C}$  for 5 min in a  $\text{H}_2$  flow atmosphere at 60 Torr. At the end of  $\text{H}_2$  annealing, one of the metalorganic sources was first introduced into the growth reactor, and the other was introduced to initiate the CdTe growth when the substrates were cooled to the growth temperature.

The surface structures of GaAs substrates at each stage prior to growth were examined by XPS and AES. The stages are (1) a chemically etched GaAs surface, (2) a  $\text{H}_2$  annealed GaAs surface in the growth reactor in the presence of residual CdTe deposits, (3) a GaAs surface exposed to DETe, and (4) a GaAs surface exposed to DMCD.  $\text{H}_2$  annealing of the etched GaAs in a clean quartz tube was also carried out to examine the effect of a  $\text{H}_2$  atmosphere on the GaAs surface structure. XPS spectra were obtained with a Surface Science Instrument SSX-100 system using monochromatized  $\text{AlK}\alpha$  radiation (1486.6 eV). The AES measurements were performed with a JEOL JAMP-10S system. The base pressure in both the XPS and AES chambers was  $1 \times 10^{-10}$  Torr. Since the samples were inevitably exposed to the laboratory air during the transport into the analyzer chamber for a few seconds to minutes, careful sputter cleaning by  $\text{Ar}^+$  ion was carried out to remove the adsorbed carbon and oxygen atoms without significantly changing the surface structure. Sputtering conditions were optimized in a series of preliminary studies. For this experiment, all XPS spectra were measured after the sputtering at 3 keV for 30 s. On the other hand,  $\text{Ar}^+$  sputtering in the AES system was carried out at 1 keV.

The growth orientations and the surface morphologies of the CdTe layers were examined by x-ray Laue back reflection patterns and Nomarski microphotographs, respectively.

### III. EXPERIMENTAL RESULTS

#### A. Surface structure of chemically etched GaAs

Figure 1(a) shows an XPS spectrum of the GaAs surface after chemical etching. An XPS spectrum of the GaAs surface after sputtering of the surface region is also shown in Fig. 1(b), which is considered a stoichiometric GaAs surface. No oxidation of Ga and As was detected at the etched GaAs surface due to the absence of XPS peaks corresponding to oxide formation.<sup>19,22,23</sup> The XPS integrated intensity ratios of As 3p to Ga 3p peaks ( $I_{\text{As}}/I_{\text{Ga}}$ ) are also shown in the figure. For the stoichiometric GaAs surface, the ratio is estimated to be 1.00. The  $I_{\text{As}}/I_{\text{Ga}}$  ratio in an etched GaAs surface is, however, larger than that for the stoichiometric surface. This indicates that after  $\text{H}_2\text{SO}_4:\text{H}_2\text{O}_2:\text{H}_2\text{O}$  etching, the GaAs surface becomes an As-rich condition by the preferential etch of Ga atoms.

A similar trend was also observed in AES analysis. Figure 2 shows an AES depth profile of the normalized As/Ga

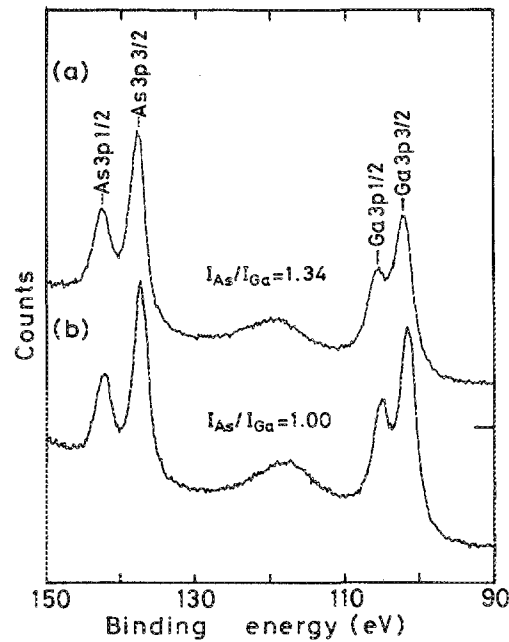


FIG. 1. Ga 3p and As 3p XPS spectra of GaAs surfaces; (a) after  $\text{H}_2\text{SO}_4:\text{H}_2\text{O}_2:\text{H}_2\text{O}$  etching, (b) after sputtering off the surface region in an etched GaAs.  $I_{\text{As}}/I_{\text{Ga}}$  shows the integrated intensity ratio of As 3p to Ga 3p.

ratios after removal of the adsorbed carbon and oxygen atoms. The As/Ga ratio is characterized by the low-energy Auger data (GaM<sub>VV</sub> 55 eV, AsM<sub>VV</sub> 31 eV), denoted by Lo, and the high-energy data (GaL<sub>M</sub>M 1070 eV, AsL<sub>M</sub>M 1228 eV), denoted by Hi. As shown in the figure, the low-energy As/Ga ratio near the surface is larger than unity while the high-energy As/Ga ratio is nearly equal to unity. The low-energy Auger data are more sensitive to the direct surface of the investigated sample, while the high-energy data give information on the more bulklike part of the sample. These results are indicative of an As-rich condition of the GaAs surface. From both XPS and AES results, it is concluded that a  $\text{H}_2\text{SO}_4:\text{H}_2\text{O}_2:\text{H}_2\text{O}$  etch leads a GaAs surface to an As-rich one with no oxide layer.

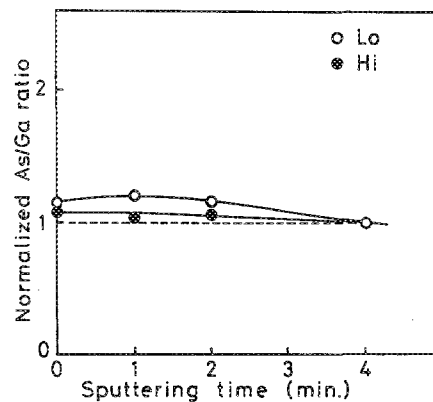


FIG. 2. AES depth profile of the normalized As/Ga ratio after removal of the adsorbed C and O atoms. The ratio is characterized by the low-energy Auger peaks (GaM<sub>VV</sub> 55 eV, AsM<sub>VV</sub> 31 eV) denoted by Lo, and the high-energy Auger peaks (GaL<sub>M</sub>M 1070 eV, AsL<sub>M</sub>M 1228 eV) denoted by Hi.

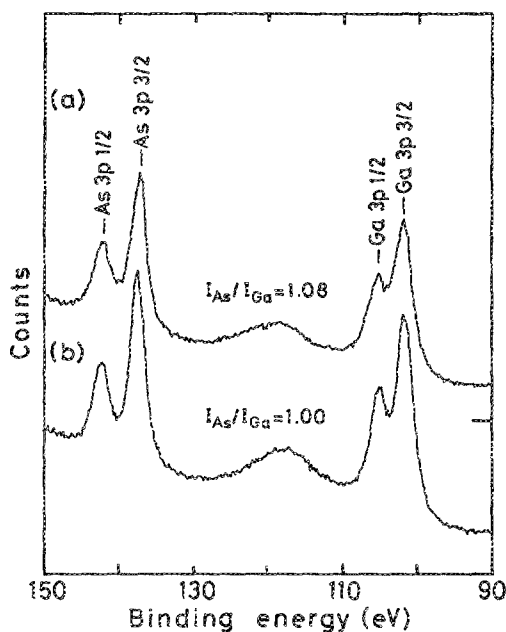


FIG. 3. Ga 3*p* and As 3*p* XPS spectra of GaAs surfaces; (a) H<sub>2</sub> annealed in a clean quartz tube after chemical etching, (b) the same GaAs surface in Fig. 1(b).  $I_{As}/I_{Ga}$  shows the integrated intensity ratio of As 3*p* to Ga 3*p*.

### B. Effect of H<sub>2</sub> annealing on the etched GaAs surface structure

Figure 3(a) shows an XPS spectrum of the GaAs surface after H<sub>2</sub> annealing in a clean quartz tube, where 3(b) represents a stoichiometric surface in Fig. 1(b). After H<sub>2</sub> annealing, the integrated intensity ratio of As 3*p* to Ga 3*p* decreases with respect to that in Fig. 1(a) and approaches unity for the stoichiometric surface. This indicates that the surface stoichiometry of the etched GaAs is recovered by the annealing in a H<sub>2</sub> flow atmosphere. A similar trend was also confirmed by AES measurement.

### C. Variation of GaAs surface structures after exposure to precursors

Figures 4(a)–4(c) show the XPS spectra of GaAs surfaces after the following procedures; (a) H<sub>2</sub> annealing in the growth reactor, (b) exposure to DETe after the annealing, and (c) exposure to DMCD after the annealing. When annealed in the growth reactor, Te atoms were adsorbed on the GaAs surface. The adsorption of Te atoms is ascribed to the decomposition of the residual CdTe deposits in the growth reactor, whereas Cd atoms were not adsorbed. Compared with Fig. 4(a), an increase in the Te signal intensity was observed after exposure to DETe, as shown in Fig. 4(b). The XPS peaks of both Ga and As could be observed although the supply of DETe was sufficient to grow a thick (~1300 Å) CdTe layer if DMCD was allowed to simultaneously flow into the growth reactor. This indicates that the amount of adsorbed Te is less than a few monolayers. The precise thickness of the adsorbed Te layer will be discussed later.

In contrast to this, an interesting result was obtained after the exposure to DMCD, as shown in Fig. 4(c). The adsorption of Cd could be seen, however its amount was less than that of Te in spite of the flow of DMCD alone, since the

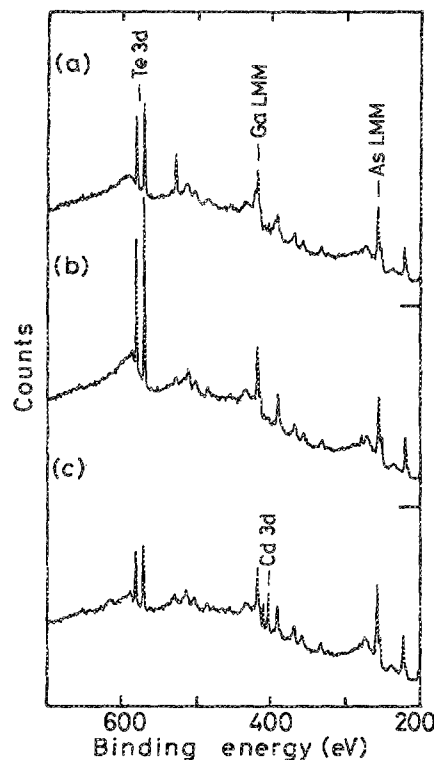


FIG. 4. XPS spectra of GaAs surfaces; (a) H<sub>2</sub> annealed in the growth reactor after chemical etching, (b) exposed to DETe after H<sub>2</sub> annealing, (c) exposed to DMCD after H<sub>2</sub> annealing.

intensity ratio of Cd 3*d* 5/2 to Te 3*d* 5/2 is estimated to be 83% for the stoichiometric CdTe surface.<sup>24</sup> This adsorption of Te atoms is also attributed to the residual CdTe deposits, which is similar to the case in Fig. 4(a). However, the amount of adsorbed Te, originating from the residual CdTe deposits, differs between Figs. 4(a) and 4(c). It is considered that this depends upon the amount of residual CdTe deposits in the growth reactor. Apparently, the amount of adsorbed Te in Fig. 4(c) is smaller than that of Te in Fig. 4(b). These adsorption characteristics were very consistent with the results of Feldman *et al.*<sup>16</sup>

### D. Orientation of CdTe grown layers

CdTe layers obtained in the case of the first supply of DETe were reproducibly (100) oriented. Pyramidal hillocks were observed on the (100) CdTe surface, which is characteristic of the surface morphology in the (100) orientation.<sup>2,25</sup> In contrast to this, when the DMCD was first introduced, CdTe layers were (100) oriented, but contained (111) oriented regions. The surface morphology of the (111) region was dusty and similar to that of the grown layer on (111)A CdTe substrate, which is characteristic of three-dimensional (3D) growth, involving double positioning type twins. From these results, it is suggested that the first metalorganic source introduced into the growth reactor is a key factor for the control of the growth orientation.

## IV. DISCUSSION

First we will discuss the difference in GaAs surface structures prior to growth between MOVPE and MBE pro-

cesses. As a result of the etching process, it is concluded that the GaAs surface becomes As-rich after the  $\text{H}_2\text{SO}_4:\text{H}_2\text{O}_2:\text{H}_2\text{O}$  etching. This result is consistent with previous reports.<sup>11,19</sup> The  $\text{H}_2\text{SO}_4:\text{H}_2\text{O}_2:\text{H}_2\text{O}$  etching is generally believed to produce a thin surface-oxide layer acting as a passivation layer.<sup>26,27</sup> However, as shown in Fig. 1(a), the rinse in deionized water after etching does not produce any passivating oxide layer on the surface, which is consistent with Massies and Contour.<sup>19</sup> They have demonstrated that oxidized phases appear as a result of the contact of the etched surface with air and are enhanced by the indium soldering at 160 °C, which is commonly performed in the MBE process.

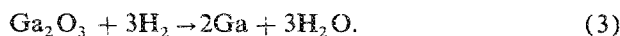
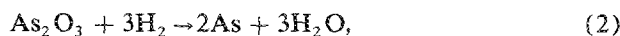
When the etched GaAs is annealed in a  $\text{H}_2$  flow atmosphere [Fig. 2(a)], the surface stoichiometry of GaAs is recovered. This suggests that excess As atoms at the As-rich GaAs surface may be preferentially desorbed in the form of  $\text{AsH}_3$  by the following reaction,



Our preliminary studies confirmed a similar effect in  $\text{H}_2$  annealing of the etched CdTe.<sup>24</sup> The CdTe surface becomes Te-rich after Br-methanol etching. However, the surface stoichiometry is recovered by  $\text{H}_2$  annealing at 450 °C. From the above results, it is concluded that the growth of the CdTe layer starts on the stoichiometric GaAs surface in our MOVPE growth experiment.

It is worthwhile to note the difference in thermal cleaning processes of GaAs substrates between MBE and MOVPE. In MBE, thermal cleaning of the etched GaAs is usually carried out under vacuum or As pressure between 570 and 600 °C to remove the oxide layer, where the As oxide and the Ga oxide are desorbed above 350 and 570 °C, respectively.<sup>19,23,26,28,29</sup> As was reported by Cho<sup>30</sup> and Srinivasa, Panish, and Temkin<sup>8</sup> in GaAs epitaxy by MBE, the (100) GaAs surface structures depend upon the substrate temperature and the ratio of the As to Ga intensity in the molecular beam. In the case of a constant substrate temperature, there is a transition from the As-stabilized to the Ga-stabilized surface with a decrease in the  $\text{As}_2/\text{Ga}$  ratio. For a given  $\text{As}_2/\text{Ga}$  ratio, the same transition can be achieved by increasing substrate temperature. In other words, high-temperature treatment leads to a deviation from the stoichiometry by a preferential loss of As. It is, therefore, considered that thermal cleaning under vacuum produces an As-deficient or a Ga-stabilized (100) GaAs surface. On the other hand, thermal cleaning under As pressure produces an As-stabilized (100) surface.<sup>8,19</sup>

In the MOVPE process, as shown in Fig. 2(a), the oxidation of the GaAs surface does not occur after chemical etching only if the etched GaAs is immediately loaded into the growth reactor. Even if the oxides exist on the surface, it is considered that they are removable by  $\text{H}_2$  annealing at 500 °C. The following deoxidizing reactions are proposed,



Thus, the use of deoxidizing  $\text{H}_2$  gas in MOVPE thermal cleaning has the significant effect of deoxidizing the surface

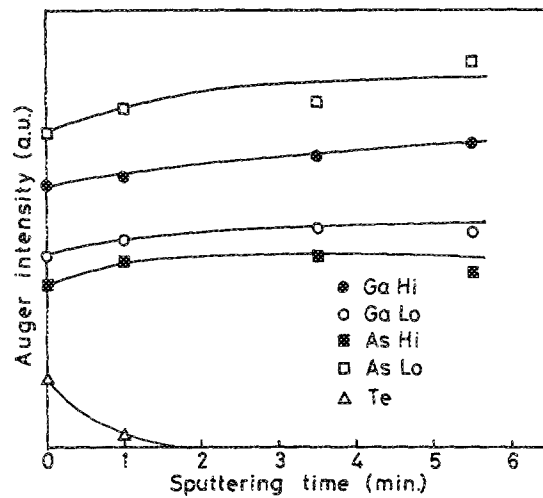


FIG. 5. AES depth profile of GaAs surface exposed to DETe in the growth reactor. This profile was obtained after removal of the adsorbed C and O atoms.

oxide below the temperature used for oxide desorption in MBE. In addition, the GaAs surface after  $\text{H}_2$  annealing is considered a Ga-stabilized one, due to a preferential loss of As. A Ga-stabilized surface is self-consistent with the adsorption characteristics of Te and Cd atoms on GaAs, as will be discussed later.

Next, let us note the variations of GaAs surface structures after the exposure to metalorganic sources. When the DETe is first introduced into the growth reactor after  $\text{H}_2$  annealing, the adsorption of Te atoms occurs on the stoichiometric GaAs surface [Fig. 4(b)]. In order to estimate a precise thickness of the adsorbed Te layer, a semiquantitative analysis was performed using Auger signal intensities of Ga and As. Figure 5 shows an AES depth profile of the GaAs surface after exposure to DETe at 420 °C in the growth reactor. This profile is traced after removal of the adsorbed carbon and oxygen atoms. As previously mentioned, the low- and high-energy Auger signals of Ga and As are denoted by Lo and Hi, respectively. For the estimate of Te coverage, two-step data is required with no C coverage (0 min) and with no Te coverage (after 3.5 min). Using Auger intensities of Ga high-energy electrons with an escape depth of approximately 17 Å,<sup>31</sup> we obtained the precise thickness of Te coverage with a value of 1.8 Å, on the assumption that the GaAs surface is simply covered by Te atoms alone. This value of Te coverage is approximately in agreement with a thickness of one monolayer of  $\text{Ga}_2\text{Te}_3$ .  $\text{Ga}_2\text{Te}_3$  forms a zincblende structure with a lattice constant of 5.88 Å. Using a value of 2.55 Å for the Ga—Te bond length in  $\text{Ga}_2\text{Te}_3$ , we can estimate that the adsorbed Te plane is located at approximately 1.6 Å up to (100) Ga-stabilized surface. It is, therefore, concluded that the GaAs surface is completely covered by one monolayer of Te after exposure to DETe during the cooling process. A Ga-stabilized surface after  $\text{H}_2$  annealing is reasonable given the chemical bonding characteristics of Te atoms, rather than Cd, easily adsorbing on the GaAs surface. This is ascribed to Ga—Te bonding.

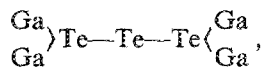
On the other hand, when the DMCD is first introduced into the growth reactor, the adsorption of both Cd and Te

TABLE I. The XPS integrated intensity ratios of As 3p to Ga 3p in Fig. 3(a), Fig. 4(b) and (c) GaAs surfaces.

	$I_{As}/I_{Ga}$
H <sub>2</sub> annealing in a clean quartz tube (Fig. 3(a))	1.08
Exposure to DETe (Fig. 4(b))	0.83
Exposure to DMCd (Fig. 4(c))	1.20

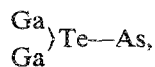
atoms occurs on the GaAs surface [Fig. 4(c)]. The amount of adsorbed Cd is, however, smaller than that of adsorbed Te. In addition, the amount of Te in this case is less than one monolayer of Te which is adsorbed in the case of exposure to DETe. It is, therefore, proposed that the GaAs surface is incompletely covered by Te atoms on which Cd atoms are partly adsorbed. As shown in Fig. 4(b), since the XPS signals of Ga and As can be detected in spite of the sufficient supply of DETe, it is suggested that the sticking coefficient of the first monolayer of Te on the (100) GaAs is high but decreases rapidly with subsequent monolayers, thereby limiting the adsorption of Te atoms to one monolayer. On the other hand, the sticking coefficient for Cd is zero on the thermally annealed GaAs surface, however, it becomes finite when Te atoms are present, as shown in Fig. 4(c).

From the above results, we will tentatively argue with the initial growth mechanism of CdTe layer on (100) GaAs substrate. For the assessment of the adsorption site of Te and Cd atoms, the XPS integrated intensity ratios of As 3p to Ga 3p in Figs. 3(a), 4(b), and 4(c) are shown in Table I. In the case of the first supply of DETe [Fig. 4(b)], a decrease in the As/Ga ratio with respect to that for H<sub>2</sub> annealing in Fig. 3(a) indicates that Te atoms are adsorbed on the Ga-stabilized (100) surface, locating over an As site. It is, therefore, suggested that a twin tetrahedral structure,



which is proposed by Cohen-Solal, Bailly, and Barbe<sup>32</sup> in MBE (100) growth, may be formed at the interfacial layer and give rise to preferential (100) growth.

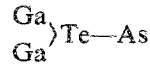
On the other hand, when the DMCd was first introduced [Fig. 4(c)], a decrease in the As/Ga ratio could not be observed. The As/Ga ratio is variable, depending upon the amount of residual CdTe deposits in the growth reactor. Since our CdTe growth starts on the stoichiometric GaAs surface, the initial growth mechanism of



a tetrahedral structure on an As-deficient (100) surface, which is proposed in MBE (111)B growth,<sup>32</sup> is not applicable to this case. Our (111)A orientation may be attributed to the island growth of CdTe at the initial stage, taking into account the incomplete coverage of Te on the GaAs surface.

It should be noted that the growth mode of (111) CdTe layer on (100) GaAs differs between MBE and our MOVPE. The MBE-grown (111) CdTe layer is (111)B oriented, involving lamella twins, and its surface morphology is specular to the eye.<sup>2,25,33</sup> We consider that this difference

significantly originates from the GaAs surface structure after the thermal cleaning. As previously described, the surface structure strongly depends upon a combination of the temperature and the ambient atmosphere in thermal cleaning. If a GaAs surface is As deficient and rough, (111)B CdTe layers are obtained in the



formation model. If a GaAs surface is stoichiometric (Ga stabilized or As stabilized), (100) CdTe layers are obtainable. On the other hand, in our MOVPE, a stoichiometric GaAs surface is formed after H<sub>2</sub> annealing at 500 °C. Therefore, the growth orientations of CdTe layers are significantly determined by the amount of Te adsorbed on the GaAs surface. The incomplete coverage of Te leads to (111)A 3D growth. The adsorption of one monolayer of Te leads to (100) growth. (111)B CdTe growth may possibly occur in MOVPE if the thermal cleaning of GaAs substrates is carried out above 580 °C and the surface becomes rough.<sup>17</sup>

## V. CONCLUSIONS

We have demonstrated the variations of the surface structures of GaAs substrates at the initial stage of CdTe MOVPE growth using XPS and AES. The GaAs surface was in an As-rich condition after H<sub>2</sub>SO<sub>4</sub>:H<sub>2</sub>O<sub>2</sub>:H<sub>2</sub>O etching. No oxidation of Ga and As was observed. The surface stoichiometry was recovered after annealing at 500 °C in a H<sub>2</sub> flow atmosphere. When the DETe was first introduced into the growth reactor after H<sub>2</sub> annealing, one monolayer of Te were adsorbed on the GaAs surface. The thickness of the adsorbed Te layer was estimated to be about 1.8 Å, which approximately corresponds to one monolayer of Ga<sub>2</sub>Te<sub>3</sub>. On the other hand, when the DMCd was first introduced, the GaAs surface was incompletely covered by Te atoms that originated from the residual CdTe deposits in the growth reactor. Cd atoms could adsorb only on the adsorbed Te atoms. It was confirmed that the first metalorganic source introduced into the growth reactor after H<sub>2</sub> annealing determines the growth orientation of the resultant CdTe layer. The first supply of DETe reproducibly leads to (100) growth while the first supply of DMCd partly leads to (111) growth. The (111) CdTe regions were (111)A oriented, which is ascribed to the island growth of CdTe.

## ACKNOWLEDGMENTS

The authors are grateful to Tosoh Akzo Co. for supplying DMCd and DETe. They are also indebted to Dr. H. Takagi and Professor K. Tanaka for carrying out the XPS measurements, and to Y. Fujimoto for the AES measurements.

<sup>1</sup>S. J. C. Irvine, J. S. Gough, J. Giess, M. J. Gibbs, A. Royle, C. A. Taylor, G. T. Brown, A. M. Keir, and J. B. Mullin, *J. Vac. Sci. Technol. A* 7, 285 (1989).

<sup>2</sup>H. Shtrikman, M. Oron, A. Raizman, and G. Cinader, *J. Electron. Mater.* 17, 105 (1988).

<sup>3</sup>G. Monfroy, S. Sivanathan, J. P. Fauric, and J. L. Reno, *J. Vac. Sci. Technol. A* 7, 329 (1989).

<sup>4</sup>R. Bean, K. Zanio, and J. Ziegler, *J. Vac. Sci. Technol. A* 7, 343 (1989).

<sup>5</sup>J. Cibert, Y. Gobil, K. Saminadayar, S. Tatarsenko, A. Chami, G. Feuillet,

- L. S. Dang, and E. Ligcoh, *Appl. Phys. Lett.* **54**, 828 (1989).
- <sup>6</sup> B. Ortner and G. Bauer, *J. Cryst. Growth* **92**, 69 (1988).
- <sup>7</sup> F. A. Ponce, G. B. Anderson, and J. M. Ballingall, *Surf. Sci.* **168**, 564 (1986).
- <sup>8</sup> R. Srinivasa, M. B. Panish, and H. Temkin, *Appl. Phys. Lett.* **50**, 1441 (1987).
- <sup>9</sup> R. D. Feldman, D. W. Kisker, R. F. Austin, K. S. Jeffers, and P. M. Bridenbaugh, *J. Vac. Sci. Technol. A* **4**, 2234 (1986).
- <sup>10</sup> R.-L. Chou, M.-S. Lin, and K.-S. Chou, *J. Cryst. Growth* **94**, 551 (1989).
- <sup>11</sup> J. P. Faurie, C. Hsu, S. Sivananthan, and X. Chu, *Surf. Sci.* **168**, 473 (1986).
- <sup>12</sup> J. M. Ballingall, M. L. Wroge, and D. J. Leopold, *Appl. Phys. Lett.* **48**, 1273 (1986).
- <sup>13</sup> N. Otsuka, L. A. Kolodzieski, R. L. Gunshor, S. Datta, R. N. Bicknell, and J. F. Schetzina, *Appl. Phys. Lett.* **46**, 860 (1985).
- <sup>14</sup> H. A. Mar, N. Salansky, and K. T. Chee, *Appl. Phys. Lett.* **44**, 898 (1984).
- <sup>15</sup> J. Cibert, K. Saminadayar, S. Tatarenko, and Y. Gobil, *Phys. Rev. B* **39**, 12047 (1989).
- <sup>16</sup> R. D. Feldman, R. F. Austin, D. W. Kisker, K. S. Jeffers, and P. M. Bridenbaugh, *Appl. Phys. Lett.* **48**, 248 (1986).
- <sup>17</sup> J. Giess, J. S. Gough, S. J. C. Irvine, J. B. Mullin, and G. W. Blackmore, *MRS Symp. Proc.* **91**, 389 (1987).
- <sup>18</sup> A. Y. Cho, *Thin Solid Films* **100**, 291 (1983).
- <sup>19</sup> J. Massies and J. P. Contour, *J. Appl. Phys.* **58**, 806 (1985).
- <sup>20</sup> S. Sone, M. Ekawa, K. Yasuda, Y. Sugiura, M. Saji, and A. Tanaka, *Appl. Phys. Lett.* **56**, 539 (1990).
- <sup>21</sup> K. Yasuda, S. Sone, M. Ekawa, Y. Sugiura, N. Matsui, A. Tanaka, and M. Saji, in *Technical Digest of the 1st International Meeting on Advanced Processing and Characterization Technologies, APCT '89*, Tokyo, Japan, 1989, pp. 131-134.
- <sup>22</sup> J. P. Contour, J. Massies, A. Saletes, and P. Staib, *Appl. Phys. A* **38**, 45 (1985).
- <sup>23</sup> P. Ainot, F. Wyczisk, and A. Friederich, *Surf. Sci.* **162**, 708 (1985).
- <sup>24</sup> K. Yasuda, Y. Iwakami, and M. Saji, in *Proceedings of the 9th International Conference on Crystal Growth*, Sendai, Japan, 1989 (to be published).
- <sup>25</sup> P. Capper, C. D. Maxey, P. A. C. Whiffin, and B. C. Easton, *J. Cryst. Growth* **96**, 519 (1989).
- <sup>26</sup> R. P. Vasquez, B. F. Lewis, and F. J. Grunthaler, *Appl. Phys. Lett.* **42**, 293 (1983).
- <sup>27</sup> J. C. M. Hwang, H. Temkin, T. M. Brennan, and R. E. Frahm, *Appl. Phys. Lett.* **42**, 66 (1983).
- <sup>28</sup> A. J. Spring Thorpe, S. J. Ingrey, B. Emmerstorfer, P. Mardevill, and W. T. Moore, *Appl. Phys. Lett.* **50**, 77 (1987).
- <sup>29</sup> G. Laurence, F. Simondet, and P. Saget, *Appl. Phys.* **19**, 63 (1979).
- <sup>30</sup> A. Y. Cho, *J. Appl. Phys.* **42**, 2074 (1971).
- <sup>31</sup> C. C. Chang, P. H. Citrin, and B. Schwartz, *J. Vac. Sci. Technol.* **14**, 943 (1977).
- <sup>32</sup> G. Cohen-Solal, F. Bailly, and M. Barbe, *Appl. Phys. Lett.* **49**, 1519 (1986).
- <sup>33</sup> P. Y. Lu, L. M. Williams, and S. N. G. Chu, *J. Vac. Sci. Technol. A* **4**, 2137 (1986).